Integrated bioprocess for conversion of gaseous substrates to liquids

Peng Hu[a,1], Sagar Chakraborty[a,1], Amit Kumar[a], Benjamin Woolston[a], Hongjuan Liu[a,2], David Emerson[a], and Gregory Stephanopoulos[a,3]

[a]Department of Chemical Engineering, Massachusetts Institute of Technology, Cambridge, MA 02139

Edited by Lonnie O. Ingram, University of Florida, Gainesville, FL, and approved January 13, 2016 (received for review August 27, 2015)

In the quest for inexpensive feedstocks for the cost-effective production of liquid fuels, we have examined gaseous substrates that could be made available at low cost and sufficiently large scale for industrial fuel production. Here we introduce a new bioconversion scheme that effectively converts syngas, generated from gasification of coal, natural gas, or biomass, into lipids that can be used for biodiesel production. We present an integrated conversion method comprising a two-stage system. In the first stage, an anaerobic bioreactor converts mixtures of gases of CO_2 and CO or H_2 to acetic acid, using the anaerobic acetogen *Moorella thermoacetica*. The acetic acid product is fed as a substrate to a second bioreactor, where it is converted aerobically into lipids by an engineered oleaginous yeast, *Yarrowia lipolytica*. We first describe the process carried out in each reactor and then present an integrated system that produces microbial oil, using synthesis gas as input. The integrated continuous bench-scale reactor system produced 18 g/L of C16-C18 triacylglycerides directly from synthesis gas, with an overall productivity of 0.19 $g{\cdot}L^{-1}{\cdot}h^{-1}$ and a lipid content of 36%. Although suboptimal relative to the performance of the individual reactor components, the presented integrated system demonstrates the feasibility of substantial net fixation of carbon dioxide and conversion of gaseous feedstocks to lipids for biodiesel production. The system can be further optimized to approach the performance of its individual units so that it can be used for the economical conversion of waste gases from steel mills to valuable liquid fuels for transportation.

two-stage bioprocess | lipid production | microbial fermentation | gas-to-liquid fuel | CO_2 fixation

Concerns over diminishing oil reserves and climate-changing greenhouse gas emissions have led to calls for clean and renewable liquid fuels (1). One promising direction has been the production of microbial oil from carbohydrate feedstocks. This oil can be readily converted to biodiesel and recently there has been significant progress in the engineering of oleaginous microbes for the production of lipids from sugars (2–5). A major problem with this approach has been the relatively high sugar feedstock cost. Alternatively, less costly industrial gases containing CO_2 with reducing agents, such as CO or H_2, have been investigated. In one application, anaerobic *Clostridia* have been used to convert synthesis gas to ethanol (6), albeit at low concentration requiring high separation cost. Here we present an alternative gas-to-lipids approach that overcomes the drawbacks of previous schemes.

We have shown previously that acetate in excess of 30 g/L can be produced from mixtures of CO_2 and CO/H_2, using an evolved strain of the acetogen *Moorella thermoacetica*, with a substantial productivity of 0.55 $g{\cdot}L^{-1}{\cdot}h^{-1}$ and yield of 92% (7). We also have demonstrated that the engineering of the oleaginous yeast *Yarrowia lipolytica* can yield biocatalysts that can produce lipids from glucose at high yields and productivities (2, 5). At the same time, as part of the quest for inexpensive feedstock, we have investigated lipid production from other substrates such as acetate and other volatile fatty acids (VFAs) that can be potentially sourced at lower costs as products of anaerobic digestion or from exhaust gases in steel manufacturing. In this study, we show that the above two systems can be integrated into a two-stage process whereby CO_2 and CO/H_2 are converted to acetic acid in the first-stage anaerobic bubble column bioreactor and the product acetic acid is subsequently converted to lipids by *Y. lipolytica* in a second-stage aerobic bioreactor. To assess the merits of this approach, we individually optimized fermentations of *M. thermoacetica and Y. lipolytica* with the intent to maximize acetate and lipid yield and productivity, respectively. A hollow fiber membrane filter was deployed in the anaerobic bioreactor to allow continuous removal of the acetic acid product and recycle of *M. thermoacetica* cells to the bubble anaerobic column. Similarly, cell recycle was also used in the second bioreactor to decouple the residence time required for growth and lipogenesis in *Y. lipolytica* cells from that of acetic acid consumption and therefore allow for the development of a dense microbial culture and high lipid concentration in the second bioreactor. We also demonstrate for the first time to our knowledge the separation of the growth phase of *M. thermoacetica* from the phase of acetic acid production: First a robust culture of *M. thermoacetica* is established in a CO-dependent growth phase by using a CO_2/CO gas mixture, and then the gas composition is switched to a H_2/CO_2 mixture that produces acetate at significantly higher specific productivity. This advance allowed us to secure both high specific productivity and a high cell density of *M. thermoacetica* for an overall very high volumetric productivity of 0.9 g of $acetate{\cdot}L^{-1}{\cdot}h^{-1}$. The two processes are then integrated in a single continuous-flow gas-to-oil processing scheme (Fig. 1), with design decisions based on the performance characteristics of the individual reactors.

Significance

In the quest for inexpensive feedstocks (cost-effective fuel production), here we show a two-stage integrated bioprocess for the conversion of syngas to lipids. We harness the innate capability of acetogens and explore concepts of gas-to-liquid mass transfer to produce an integrated two-stage bioreactor system that can convert gases to liquid fuels at scale. Additionally, as the rate of CO_2 fixation substantially exceeds that of CO_2 generation in the two units of the process, there is significant potential for CO_2 recycling in our integrated system. In a broader sense, implementation of these concepts for fuel production may extend to a number of commercially important biological platforms, depending on the potential sources of synthesis gas or its conversion products, namely, acetate.

Author contributions: G.S. designed research; P.H., S.C., and H.L. performed research; A.K., B.W., D.E., and G.S. analyzed data; and A.K. and G.S. wrote the paper.

The authors declare no conflict of interest.

This article is a PNAS Direct Submission.

See Commentary on page 3717.

[1]P.H. and S.C. contributed equally to this work.

[2]Present address: Institute of Nuclear and New Energy Technology, Tsinghua University, Beijing 100084, China.

[3]To whom correspondence should be addressed. Email: gregstep@mit.edu.

This article contains supporting information online at www.pnas.org/lookup/suppl/doi:10.1073/pnas.1516867113/-/DCSupplemental.

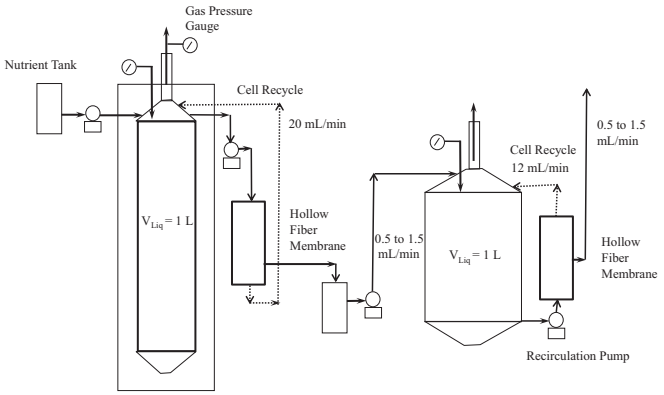

Fig. 1. Integrated bioprocess: Schematic of two-stage lipid production process using microbial conversion. In stage 1, CO_2 is fermented to a volatile fatty acid; in stage 2, this acid is converted to lipids by an engineered strain.

Results

Cell Growth and Acetate Production from Syngas. Acetic acid production from syngas by *M. thermoacetica* is shown in Fig. 2, which presents time courses for growth and acetic acid titer in an anaerobic bubble column run independently. Our prior work provided the basis for flow rates relevant to this study (7). Fermentation was carried out at a flow rate of 1,000 standard cubic centimeters per minute (sccm), using either CO or H_2 as reducing gas at a composition of 7/3 CO/CO_2 or 7/3 H_2/CO_2. Substantial amounts of acetic acid (in excess of 30 g/L) were produced under both conditions during similar time periods. Notably, the maximum cell density under H_2 (max OD of ∼2.5) was less than one-quarter of that achieved with CO (max OD of ∼11) as electron donor. Because the volumetric productivities of acetic acid were similar in these two experiments, the specific productivity of acetic acid under H_2/CO_2 was therefore four times greater than that under CO/CO_2. This difference in specific cell productivity is likely due to the energetic difference between H_2 and CO metabolism in this organism. *M. thermoacetica* generates ATP under autotrophic conditions by chemiosmosis. In this mechanism, oxidation of reduced ferredoxin by an energy-conserving hydrogenase complex (Ech) results in translocation of protons across the membrane. The generated proton gradient is used by the membrane-bound ATP synthase to generate ATP (8). Production of acetyl-CoA from H_2/CO_2 involves oxidation of 2 mol ferredoxin for every mole of acetyl-CoA synthesized, whereas production of acetyl-CoA from CO requires oxidation of 6 mol of ferredoxin. Thus, growth on CO supports more ATP production, which, in turn, translates into higher biomass concentrations. The apparent ATP limitation during growth on H_2/CO_2 forces increased diversion of acetyl-CoA from biomass synthesis to acetate production to increase ATP synthesis via substrate-level phosphorylation, resulting in higher overall acetate fluxes per unit biomass.

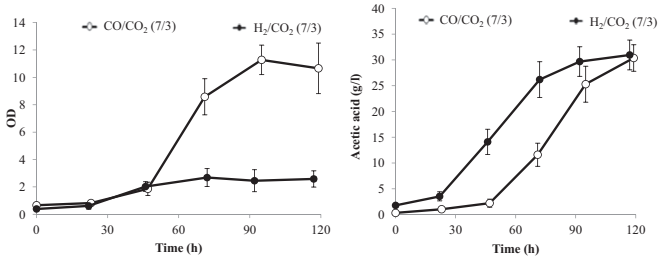

Fig. 2. Cell growth and acetic acid production using either CO or H_2 as a reducing gas at a composition of 7/3 CO/CO_2 or 7/3 H_2/CO_2 and a flow rate of 1,000 sccm. The maximum cell density under H_2 (max OD of ∼2.5) is less than one-quarter of that achieved with CO (max OD of ∼11) as electron donor. Substantial amounts of acetic acid (∼30 g/L) are produced under both conditions. SDs from triplicate runs are presented.

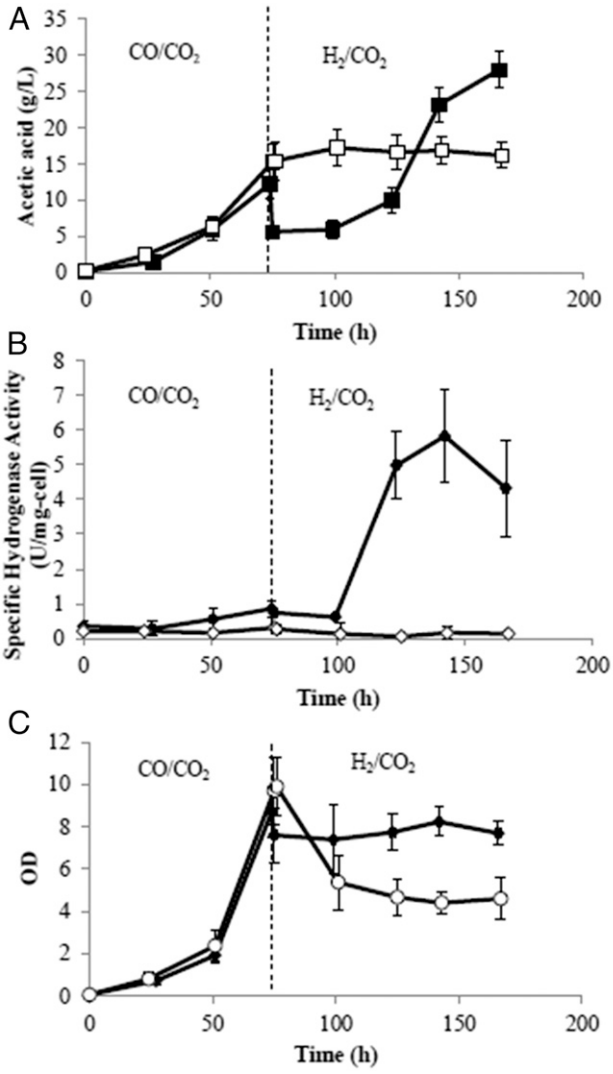

Fig. 3. (*A*–*C*) Time courses of (*A*) acetic acid concentration, (*B*) specific hydrogenase activity, and (*C*) optical density for two different methods of switching the gas composition in the anaerobic bubble column. Solid symbols are for the case in which the gas switch from CO/CO_2 (4/1) and the flow rate of 1,000 sccm to H_2/CO_2 (2/1) were performed and the same flow rate was accompanied with replacement of half of the reactor medium with fresh media. In the run represented by the open symbols a similar gas switch was carried out but without medium replacement. SDs from triplicate runs are presented.

Acetate Productivity with Gas Composition Switch and Media Replacement. As shown in the previous section, the specific productivity of acetate on H_2 by *M. thermoacetica* is about four times that achieved on CO. On the other hand, much higher cell densities can be supported by a CO/CO_2 mixture. This suggests that one should first grow the *M. thermoacetica* culture on a CO/CO_2 mixture and switch to a H_2/CO_2 composition after the culture is established to take advantage of the higher acetate specific productivity on hydrogen. An experiment was thus designed to assess whether the high cell density achievable by growth on CO/CO_2 could be harnessed for higher overall productivity by switching the gas composition to H_2/CO_2 after the initial growth phase. However, the simple switch of gas composition led to a significant decline of

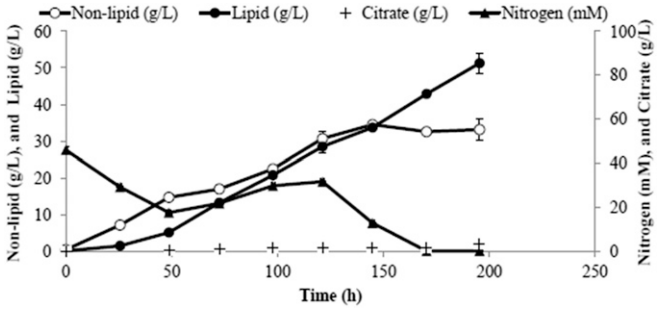

Fig. 4. Fermentation characteristics of *Y. lipolytica* in semicontinuous mode during acetic acid consumption (high strength). *Y. lipolytica* produced lipids at a titer of 51 g/L with a productivity of 0.26 $g{\cdot}L^{-1}{\cdot}h^{-1}$ and lipid content of 61%. SDs from triplicate runs are presented.

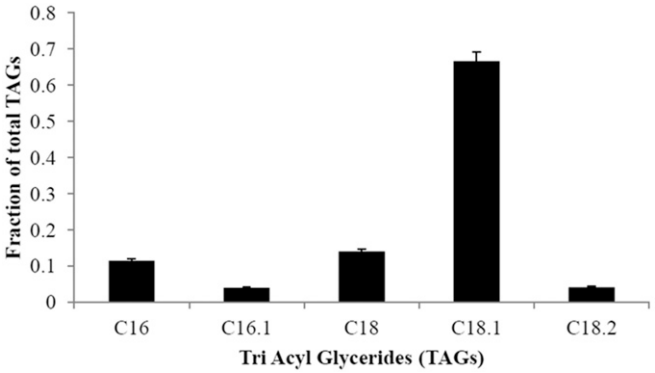

Fig. 6. Fatty acid distribution during bioreactor fermentation by using *Y. lipolytica*. C16 palmitate, C16.1 palmitoleate, C18 stearate, C18.1 oleate, and C18.2 linoleate are shown. Samples were performed in triplicate.

M. thermoacetica culture and no change in acetic acid production (Fig. 3). We hypothesized that this might be due to low hydrogenase activity at the time of the switch, which is known to be inhibited by carbon monoxide (Fig. 3*B*). Although constitutively expressed, hydrogenase activity is 18-fold higher in H_2-cultivated cells than in CO-grown cells (9), and it is required for growth on H_2 as a sole electron donor. Successful transition from CO to hydrogen without decline in cell mass and that also maintained the biosynthetic capacity of cells was achieved when half the medium was replaced with fresh medium at the same time of the gas switch. In this experiment, after an initial decline caused by the dilution from the fresh medium, cell density was stabilized (Fig. 3*C*) at the new value following the gas switch and, more importantly, maintained its acetic acid productivity. An average overall acetic acid productivity of 0.9 $g{\cdot}L^{-1}{\cdot}h^{-1}$ after the gas switch was obtained, which was 50% higher than that of 0.6 $g{\cdot}L^{-1}{\cdot}h^{-1}$ observed before the gas switch. These results are consistent with the time course of hydrogenase activity, which rose roughly 20-fold in 1 d following the replacement of CO by H_2. This experiment demonstrated that the volumetric productivity of acetic acid could be significantly improved by switching the gas composition and replacing the media midrun, relative to what was possible before using CO_2/H_2 or CO_2/CO gas alone.

Lipid Production from High-Strength Acetic Acid by *Y. lipolytica*. Lipid production from acetic acid (30% vol/vol) by *Y. lipolytica* in a fed-batch mode is shown in Fig. 4. *Y. lipolytica* produced lipids at a titer of 51 g/L with a productivity of 0.26 $g{\cdot}L^{-1}{\cdot}h^{-1}$ and lipid content of 61%, which is the highest reported to date on acetate. Fontannile et al. (10) grew *Y. lipolytica* first on glucose and then transferred to VFAs, obtaining lower productivity (0.16 $g{\cdot}L^{-1}{\cdot}h^{-1}$) compared with our study, albeit at lower lipid titers (12 g/L), conversion yields (0.13 g/g), and lipid content of 40%.

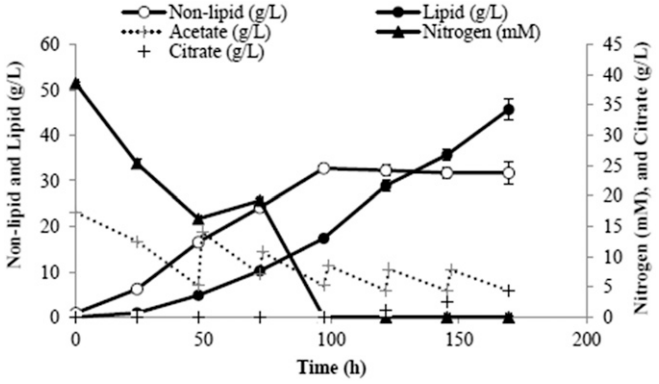

Fig. 5. Acetic acid (3% vol/vol) consumption (low strength) and lipid production by using *Y. lipolytica* in semicontinuous mode. A hollow fiber module was used to recycle cells and maintain constant volume. The time courses show a lipid titer of 46 g/L with an overall productivity of 0.27 $g{\cdot}L^{-1}{\cdot}h^{-1}$ and lipid content of 59%. SDs from triplicate runs are presented.

Lipid Production from Low-Strength Acetic Acid by *Y. lipolytica*. A dilute substrate will result in a dilute product. An exception is possible in the case of intracellular products (like lipids) and also when cells are recycled to increase their residence time in the bioreactor to allow them more time to attain higher lipid content. This can be achieved with the use of a hollow fiber membrane whereby spent medium with a low concentration of residual acetate is removed whereas cells are recycled back into the bioreactor. This scheme was implemented and Fig. 5 shows the time courses of lipid production from dilute acetic acid (3% vol/vol). A lipid titer of 46 g/L was obtained with an overall productivity of 0.27 $g{\cdot}L^{-1}{\cdot}h^{-1}$ and lipid content of 59%. An average lipid composition profile generated in this run is shown in Fig. 6. This profile is similar to that of Knothe (11), with higher fractions of unsaturated fats, which are desirable as they increase the cetane number and decrease the cloud point of the resulting biodiesel.

Carbon fluxes were calculated for this run. *Y. lipolytica* consumes acetic acid and converts the carbon to CO_2, lipids, and nonlipid biomass, with small amounts of citrate produced as a by-product. The cumulative carbon mass balance is closed to within 5%, with CO_2 accounting for 54% of the total carbon products (Fig. 7). A stoichiometric model was constructed to assess the efficiency of acetate utilization during the fermentation process, considering usual metabolic processes and associated ATP and NADPH costs for nonlipid biomass production (growth) as well as lipid production. Details of the model are provided in *SI Notes on the Model*. The model essentially predicts, for a given amount of lipid and biomass formed, the amounts of acetate required and CO_2 formed, based on reasonable assumptions about the pathways responsible for the main metabolic processes underlying growth and lipid synthesis. By substituting the experimentally measured lipid and nonlipid production data, we determined the theoretically predicted amount of acetate consumption and carbon dioxide production. Upon comparison with the respective experimentally observed levels of acetate consumption and CO_2 production it can be seen that experimental lipid production and nonlipid production are within 10% of the theoretical values, as shown in Fig. 8. This suggests that the engineered strain is well optimized for lipid synthesis, wasting very little substrate for other processes.

Integrated System for Syngas Bioconversion to Lipids. Based on the results obtained with the two bioreactor units, the integrated

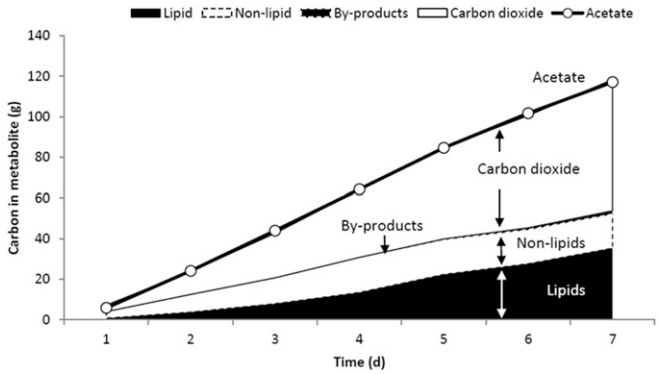

Fig. 7. Carbon balance of acetate consumption and lipid production. Shown are input carbon as acetate and output carbon (lipid, nonlipid, by-products, and CO_2). The cumulative carbon mass balance is closed to within 5%, with CO_2 accounting for 54% of the total carbon products.

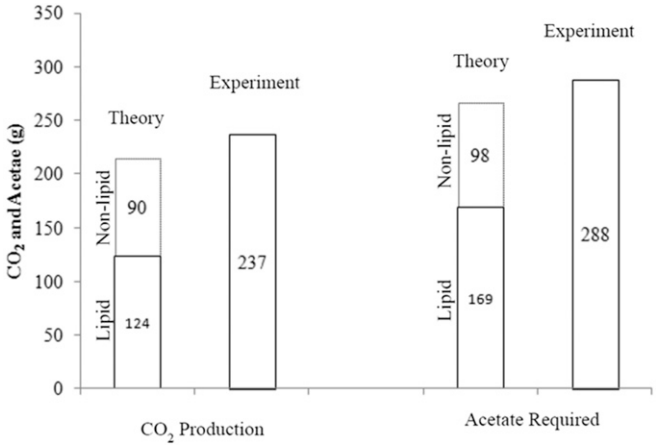

Fig. 8. Theoretical predictions and experimental values of acetate consumed and CO_2 produced. A stoichiometric model was constructed to assess the efficiency of acetate utilization during the fermentation process, taking into account acetate consumed and CO_2 produced for both nonlipid biomass production (growth) and lipid production, including the associated ATP and NADPH costs of these processes. The experimental CO_2 production and acetate consumption are within 10% of the expected theoretical values. Model detail is provided in *SI Notes on the Model*.

system of Fig. 1 was assembled and operated as shown in Table 1. Fig. 9 shows the time courses for cell growth and acetic acid production by *M. thermoacetica* in the anaerobic bubble column, with Fig. 10 summarizing the same for *Y. lipolytica* in the aerobic stirred tank bioreactor. Before 93 h (first phase), the anaerobic bioreactor was fed with a CO/CO_2 gas mixture at 1,000 sccm and composition of (4/1). During this period, *M. thermoacetica* grew to an OD of 10.3 and acetic acid accumulated to 12 g/L with a productivity of 0.4 $g{\cdot}L^{-1}{\cdot}h^{-1}$, excluding the lag phase. Then, the gas supply was changed to H_2/CO_2 at a flow rate of 1,200 sccm and composition of (2/1). The second phase lasted from 93 h to 218 h and was characterized by a steady increase of acetic acid until the maximum of 25 g/L was reached. After the gas switch, the cell OD dropped from the maximum value of 10.3 to about 8 and recovered slowly until the end of the second phase (see Fig. S1 for different media ratios). At the same time (186–218 h), ~1,000 mL liquid medium was removed from the anaerobic bioreactor through a hollow fiber membrane and fed into the aerobic bioreactor. In the third phase (after 218 h), a continuous-flow operation was initiated, which maintained the level of acetic acid in the anaerobic reactor at the maximum concentration of ~25 g/L. This was achieved by continuously removing acetic acid while recycling *M. thermoacetica* cells through a hollow fiber membrane. Cell growth was minimal during this phase and the reactor thus operated like a perfusion bioreactor. The maximum acetic acid concentration of 25 g/L was selected to prevent inhibition of further acetate production (7). The working volumes of both bioreactors were maintained constant by the addition of fresh media in the first bioreactor and removal of spent media from the aerobic bioreactor as shown in Fig. 1. The acetic acid concentration of the media reservoir was measured periodically between 118 h and 312 h, with a total of 212 g acetic acid produced in 194 h. The average productivity of acetic acid was 1.1 $g{\cdot}L^{-1}{\cdot}h^{-1}$ after the gas switch, threefold higher than the first stage when CO/CO_2 was used as gas feedstock.

The time courses of cell growth and lipids production in the aerobic bioreactor are presented in Fig. 10. Lipid titer was 18 g/L and lipid content 36%. Although these numbers are lower than those achieved in the individual units and prior studies (2), the results are nevertheless encouraging as they demonstrate the feasibility of operating an integrated gas-to-lipids process, which was the goal of this study. A comparison of the results obtained from the single-stage bioreactors and those of the combined process is provided in Table 2. The main difference between the independent lipid production run and the integrated process is the lipid yield from acetic acid. In the single-unit investigation, more acetic acid was converted to lipids, whereas in the combined process more acetic acid was converted to nonlipid biomass. In *Y. lipolytica*, the C/N ratio is known to strongly influence lipid production and titers. In the combined process, the C/N ratio was not strictly controlled and this likely impacted the yields negatively. Therefore, future experiments should aim to minimize the nitrogen content of the *M. thermoacetica* medium, which will limit the nitrogen content of the acetic acid feed to the *Y. lipolytica* reactor after the start of the lipid production phase.

Discussion

There are several new concepts deployed in this study that allowed the successful implementation of the integrated gas-to-lipids

Table 1. Experimental conditions during the integrated bioprocess run

	Anaerobic bubble column reactor			Aerobic reactor	
Phase	Time, h	Gas composition, flow rate (sccm)	Mode (liquid flow rate to aerobic reactor)	Time, h	Mode (outlet liquid flow rate)
I	0–93	CO/CO_2 (4/1), 1,000	Batch	0–93	n.s.
II	94–185	H_2/CO_2 (2/1), 1,200	Batch	0–185	n.s.
	186–218*	H_2/CO_2 (2/1), 1,200	Continuous, 0.5 mL/min	186–218	n.s.
III	219–312	H_2/CO_2 (2/1), 1,200	Continuous, 1.5 mL/min	219–314†	Continuous, 1.5 mL/min

n.s., not started.
*~1,000 mL liquid medium obtained for aerobic reactor.
†Aerobic bioreactor inoculated with *Y. lipolytica* and continuous operation started.

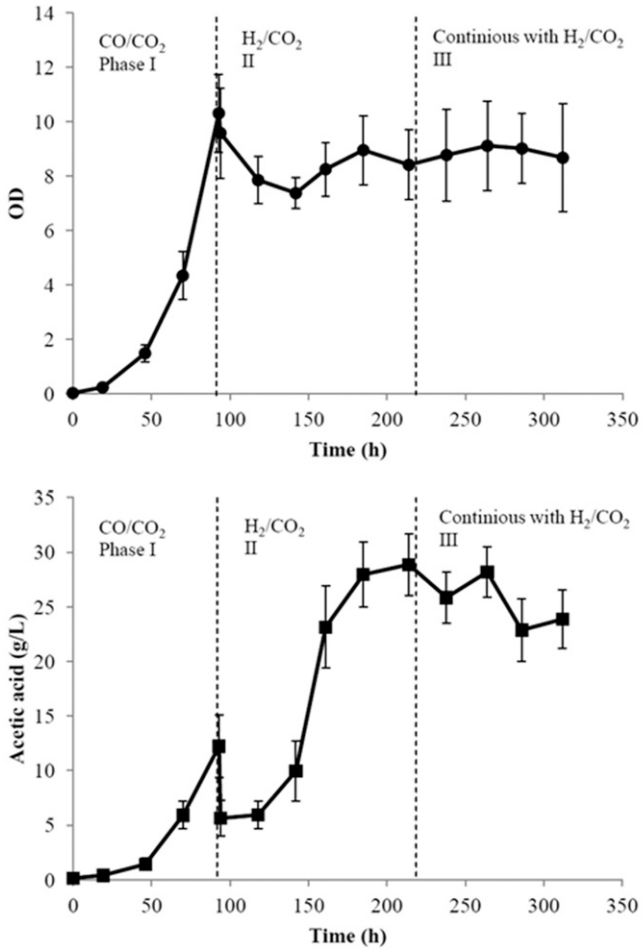

Fig. 9. Cell growth of *M. thermoacetica* and acetic acid production of the integrated fermentation experiment. In all three phases gaseous substrate is provided in continuous mode, whereas liquid as batch mode is provided in the first two phases. In the third phase both gas and liquid are in continuous mode. Successful gaseous substrate switch allowed acetic acid production (maximum concentration of ~25 g/L) in the anaerobic reactor. This is achieved by continuously removing acetic acid while recycling *M. thermoacetica* cells through a hollow fiber membrane. SDs from triplicate runs are presented.

conversion process. First, we used the acetogen *M. thermoacetica* as a model organism because of its very high autotrophic flux to acetyl-CoA, which naturally produces acetate at very high rates and almost theoretical yields via the canonical Wood–Ljungdahl pathway. Additionally, the high temperature of operation (T_{opt} 60 °C) of this thermophilic organism makes it of industrial interest as it would require less cooling of syngas before feeding the bioreactor (12) compared with the other model acetogens, *Clostridium ljungdahlii* (T_{opt} 37 °C) (13) and *Acetobacterium woodii* (T_{opt} 30 °C) (14). Our prior work with *M. thermoacetica* (7) provided the basis of acetic acid production at high rates relevant to this study.

Second, this work highlights a novel gas composition switch strategy as an important part of the process required for achieving higher overall acetate productivity. Additionally, this result points out the importance of the physiological state of *M. thermoacetica* at the time of switching the gas composition, so future experiments should aim at identifying optimal medium replacement and culture viability or alternately modifying medium composition to achieve maximum titers, yields, and productivities.

Third, as summarized in Table 2, the numbers of merit obtained for the integrated system are lower than those achieved for the individual bioreactor units. Additionally, the overall energetic efficiency (from hydrogen to lipid and yeast) of the integrated system is 34.4%, compared with maximum theoretical values of 43% (considering yeast energy content) and 60.5% (assuming only hydrogen and tripalmitin are the energy carriers). Model detail on energy efficiency calculation is provided in *SI Notes on Energy Efficiency Calculations*. Therefore, the process requires further optimization. Nitrogen control in the media of the two units is mentioned as one direction that can be pursued to this end.

Fourth, there is significant potential for reduction of CO_2 emissions in our system compared with the single-stage systems. For example, the process in the first reactor is theoretically expected to consume 100.2 mol CO_2 whereas aerobic lipid synthesis is theoretically expected to produce 49.22 mol CO_2 (a cumulative balance for the whole operation). As such, our process actually fixes CO_2 using CO and/or H_2 as reducing agents. Carbon dioxide generated in the lipid-producing aerobic reactor could be recycled and used by the anaerobic bacteria of the first stage, yielding a significant overall rate of CO_2 fixation. In the same vein, the nonlipid biomass could be used to supply the yeast extract used in the media of both reactors following extraction of the lipids.

The main limitation in biodiesel (the primary renewable alternative to diesel) production is feedstock availability and cost (15). It is unlikely that food-competing feedstocks will contribute significantly to the production of renewable transportation fuels (16). In the quest for a cheaper feedstock, synthesis gas offers attractive features. Also, steel mill gas and natural gas can be used as a cost-effective feedstock (12, 17–19). As such, a syngas-to-liquids process represents an infrastructure-compatible platform that will be important for reducing dependence on fossil fuels. The gas-to-liquid concept presented here has the potential to provide biodiesel production from CO_2 in a way that does not impose demands on or changes of land use and is not confined by the need of access to carbohydrate feedstocks.

Materials and Methods

Bacteria, Media, and Cultivation Conditions. For details on routine cultivation of microorganisms and descriptions of the strains used, see *SI Notes on Materials and Methods*.

Anaerobic Bubble Column Bioreactor Operation. *M. thermoacetica* was grown in a 1-L glass bubble column bioreactor at 60 °C. Gas composition was controlled with a four-channel mass flow controller and pH was controlled by addition of 5 N sodium hydroxide or hydrochloric acid. Prepared medium (excluding cysteine) was autoclaved, transferred to the bioreactor, and purged with oxygen-free N_2 gas overnight. pH was adjusted to 6.0 unless otherwise stated, and syngas flow was initiated and continuously bubbled

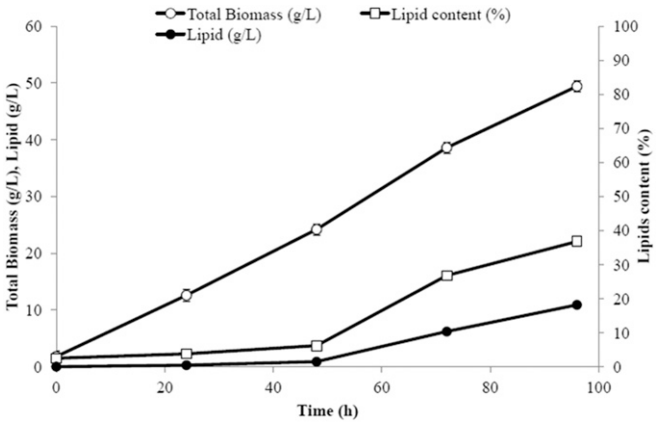

Fig. 10. Lipid titer and biomass production in an integrated process (phase III). Shown is the time course of cell growth and lipid production (18 g/L titer and 36% lipid content) in the aerobic bioreactor. SDs from triplicate runs are presented.

Table 2. A comparison of results of single-stage and integrated processes

Substrate	Microorganism	Substrate feeding mode	Product	Product titer, $g \cdot L^{-1}$ (lipid content % of dry cell weight)	Productivity, $g \cdot L^{-1} \cdot h^{-1}$	Product yield, $g \cdot g^{-1}$
Syngas	*Moorella thermoacetica*	Continuous	Acetic acid	30	0.57	NA
Acetate	*Yarrowia lipolytica*	Fed batch	Lipid	46 (59)	0.27	0.16
Syngas	Both	Continuous	Lipid	18 (36)	0.19	0.09

NA, not analyzed.

through the bioreactor (see *SI Notes on Materials and Methods* for syngas composition). A cysteine solution was added to the medium to remove residual oxygen, and the bioreactor was inoculated at 5% vol/vol.

Stirred Tank Aerobic Bioreactor Conditions. *Y. lipolytica* was grown in a 2-L stirred tank bioreactor. Dissolved oxygen (DO) was controlled to 20% saturation, and pH was controlled to 7.3 by addition of acetic acid. During the first 70 h of growth, the feed consisted of 3% acetic acid and 15 g/L ammonium sulfate to provide sufficient nitrogen for generation of nonlipid biomass. Thereafter the feed consisted solely 3% vol/vol acetic acid. Additional acetate required to maintain an acetate concentration of ∼15 g/L was provided as a sodium acetate solution (300 g/L). A hollow fiber module was used to recycle cells and maintain constant volume (20). A theoretical maximum of carbon accumulation is determined as lipid and nonlipid production on acetate (21, 22).

Integrated Bioprocess System. The bubble column bioreactor (for *M. thermoacetica*) and stirred tank bioreactor (for *Y. lipolytica*) were integrated in a process shown schematically in Fig. 1. Experimental conditions during integrated bioprocess run are provided in Table 1, and the complete operation is described in *SI Notes on Materials and Methods*. Briefly, the bubble column was operated first in a batch mode with respect to the liquid phase. Following the switch of syngas composition and the attainment of stationary phase, continuous liquid removal was initiated and cells were recycled via a hollow fiber membrane. After 1 L effluent had been transferred, the aerobic bioreactor was inoculated and operated continuously, again with cell recycling accomplished via a hollow fiber membrane.

Fermentation Analytics. Effluent gas composition was analyzed via microGC-TCD (gas chromatography–thermal conductivity detector). Acetate and citrate were measured via HPLC with refractive index detector (RID) detection. Growth was monitored via OD_{600} for *M. thermoacetica* (23) and gravimetrically for *Y. lipolytica*. Conversion of OD to dry cell weight was via ratios determined in our laboratory. Total lipids were quantified using a modified version of a direct transesterification protocol adapted from US Patent 7932077 (24) and Griffiths et al. (25), using gas chromatography–flame ionization detector (GC-FID). For details see *SI Notes on Materials and Methods*.

Hydrogenase Assay. Hydrogenase activity was assayed anaerobically by standard protocols following the reduction of benzyl viologen with permeabilized cells in a sealed cuvette (26, 27). For details see *SI Notes on Materials and Methods*.

ACKNOWLEDGMENTS. We thank Dr. Victoria Bertics and Dr. Peter Girguis (Harvard University) for their help. This research was supported by an ARPA-E grant of the Electrofuels program (Award DE-AR0000059) and the Department of Energy's Genomic Science Program (Grant DE-SC0008744) (MIT: 692-6611).

1. Chu S, Majumdar A (2012) Opportunities and challenges for a sustainable energy future. *Nature* 488(7411):294–303.
2. Tai M, Stephanopoulos G (2013) Engineering the push and pull of lipid biosynthesis in oleaginous yeast *Yarrowia lipolytica* for biofuel production. *Metab Eng* 15:1–9.
3. Blazeck J, et al. (2014) Harnessing *Yarrowia lipolytica* lipogenesis to create a platform for lipid and biofuel production. *Nat Commun* 5:3131.
4. Liu L, Pan A, Spofford C, Zhou N, Alper HS (2015) An evolutionary metabolic engineering approach for enhancing lipogenesis in *Yarrowia lipolytica*. *Metab Eng* 29:36–45.
5. Qiao K, et al. (2015) Engineering lipid overproduction in the oleaginous yeast *Yarrowia lipolytica*. *Metab Eng* 29:56–65.
6. Shen Y, Brown R, Wen Z (2014) Enhancing mass transfer and ethanol production in syngas fermentation of *Clostridium carboxidivorans* P7 through a monolithic biofilm reactor. *Appl Energy* 136:68–76.
7. Hu P, Rismani-Yazdi H, Stephanopoulos G (2013) Anaerobic CO2 fixation by acetogenic bacterium *Moorella thermoacetica*. *AICHE* 59:3176–3183.
8. Schuchmann K, Müller V (2014) Autotrophy at the thermodynamic limit of life: A model for energy conservation in acetogenic bacteria. *Nat Rev Microbiol* 12(12):809–821.
9. Daniel SL, Hsu T, Dean SI, Drake HL (1990) Characterization of the H_2- and CO-dependent chemolithotrophic potentials of the acetogens *Clostridium thermoaceticum* and *Acetogenium kivui*. *J Bacteriol* 172(8):4464–4471.
10. Fontanille P, Kumar V, Christophe G, Nouaille R, Larroche C (2012) Bioconversion of volatile fatty acids into lipids by the oleaginous yeast *Yarrowia lipolytica*. *Bioresour Technol* 114:443–449.
11. Knothe G (2009) Improving biodiesel fuel properties by modifying fatty ester composition. *Energy Environ Sci* 2:759–766.
12. Abubackar HN, Veiga MC, Kennes C (2011) Biological conversion of carbon monoxide: Rich syngas or waste gases to bioethanol. *Biofuels Bioprod Biorefin* 5:93–114.
13. Tanner RS, Miller LM, Yang D (1993) *Clostridium ljungdahlii* sp. nov., an acetogenic species in clostridial rRNA homology group I. *Int J Syst Bacteriol* 43(2):232–236.
14. William EB, Schoberth S, Tanner RS, Wolfe RS (1997) *Acetobacterium*, a new genus of hydrogen-oxidizing, carbon dioxide-reducing, anaerobic bacteria. *Int J Syst Evol Microbiol* 27:355–361.
15. Papoutsakis ET (2015) Re-assessing the progress in the production of advanced biofuels in the current competitive environment and beyond: What are the successes and where progress eludes us and why. *Ind Eng Chem Res* 54:10170–10182.
16. Hill J, Nelson E, Tilman D, Polasky S, Tiffany D (2006) Environmental, economic, and energetic costs and benefits of biodiesel and ethanol biofuels. *Proc Natl Acad Sci USA* 103(30):11206–11210.
17. Köpke M, Mihalcea C, Bromley JC, Simpson SD (2011) Fermentative production of ethanol from carbon monoxide. *Curr Opin Biotechnol* 22(3):320–325.
18. Wilkins MR, Atiyeh HK (2011) Microbial production of ethanol from carbon monoxide. *Curr Opin Biotechnol* 22(3):326–330.
19. Nybo SE, Khan NE, Woolston BM, Curtis WR (2015) Metabolic engineering in chemolithoautotrophic hosts for the production of fuels and chemicals. *Metab Eng* 30:105–120.
20. Chakraborty S (2013) Exploring volatile fatty acids (VFAs) as a novel substrate for microbial oil production. Thesis (Massachusetts Institute of Technology, Cambridge, MA).
21. von Stockar U, Liu J (1999) Does microbial life always feed on negative entropy? Thermodynamic analysis of microbial growth. *Biochim Biophys Acta* 1412(3):191–211.
22. Fei Q, et al. (2011) The effect of volatile fatty acids as a sole carbon source on lipid accumulation by Cryptococcus albidus for biodiesel production. *Bioresour Technol* 102(3):2695–2701.
23. Seifritz C, Fröstl JM, Drake HL, Daniel SL (2002) Influence of nitrate on oxalate- and glyoxylate-dependent growth and acetogenesis by *Moorella thermoacetica*. *Arch Microbiol* 178(6):457–464.
24. Damude HG, et al. (2011) High eicosapentaenoic acid producing strains of *Yarrowia lipolytica*. E. I. Du Pont De Nemours & Co., assignee. Patent US7932077 B2. 26 (April 2011).
25. Griffiths MJ, van Hille RP, Harrison STL (2010) Selection of direct transesterification as the preferred method for assay of fatty acid content of microalgae. *Lipids* 45(11):1053–1060.
26. Xu D, Lewis RS (2012) Syngas fermentation to biofuels: Effects of ammonia impurity raw syngas on hydrogenase activity. *Biomass Bioenergy* 45:303–310.
27. Wang S, Huang H, Kahnt J, Thauer RK (2013) A reversible electron-bifurcating ferredoxin- and NAD-dependent [FeFe]-hydrogenase (HydABC) in *Moorella thermoacetica*. *J Bacteriol* 195(6):1267–1275.
28. Berg JM, Tymoczko JL, Stryer L (2006) *Biochemistry* (Freeman, New York), 6th Ed.
29. van Milgen J (2002) Modeling biochemical aspects of energy metabolism in mammals. *J Nutr* 132(10):3195–3202.
30. Shuler ML, Kargi F (2001) *Bioprocess Engineering: Basic Concepts* (Prentice Hall, New Jersey), 2nd Ed.
31. Verduyn C (1991) Physiology of yeasts in relation to biomass yields. *Antonie van Leeuwenhoek* 60(3–4):325–353.